



Published in final edited form as:

J Orthop Res. 2021 August ; 39(8): 1800–1810. doi:10.1002/jor.24781.

Increased volume and collagen crosslinks drive soft tissue contribution to post-traumatic elbow contracture in an animal model

Chelsey L. Dunham¹, Heiko Steenbock², Jürgen Brinckmann^{2,3}, Alex J. Reiter⁴, Ryan M. Castile⁴, Aaron M. Chamberlain⁵, Spencer P. Lake^{1,4,5}

¹Department of Biomedical Engineering, Washington University in St. Louis, MO;

²Institute of Virology and Cell Biology, University of Lübeck, Germany;

³Department of Dermatology, University of Lübeck, Germany;

⁴Department of Mechanical Engineering, Washington University in St. Louis, MO;

⁵Department of Orthopaedic Surgery, Washington University in St. Louis, MO

Abstract

Post-traumatic joint contracture (PTJC) in the elbow is a biological problem with functional consequences. Restoring elbow motion after injury is a complex challenge because contracture is a multi-tissue pathology. We previously developed an animal model of elbow PTJC using Long-Evans rats and showed that the capsule and ligaments/cartilage were the primary soft tissues that caused the persistent joint motion loss. The objective of this study was to evaluate tissue specific changes within the anterior capsule and lateral collateral ligament (LCL) that led to their contribution to elbow contracture. In our rat model of elbow PTJC, a unilateral surgery replicated damage that commonly occurs due to elbow dislocation. Following surgery, the injured limb was immobilized for 42 days. The capsule and LCL were evaluated after 42 days of immobilization or 42 days of immobilization followed by 42 days of free mobilization. We evaluated extracellular matrix protein biochemistry, non-enzymatic collagen crosslink content, tissue volume with contrast enhanced micro-computed tomography, and tissue mechanical properties. Increased collagen content, but not collagen density, was observed in both injured limb capsules and LCLs, which was consistent with the increased tissue volume. Injured limb LCLs exhibited decreased normalized maximum force, and both tissues had increased immature collagen crosslinks compared to control. Overall, increased tissue volume and immature collagen crosslinks in the capsule and LCL drive their contribution to elbow contracture in our rat model.

Keywords

Elbow; Post-traumatic Contracture; Collagen Crosslinks; Capsule; Lateral Collateral Ligament

Corresponding author: Spencer P. Lake; Address: 1 Brookings Drive, Campus Box 1185, St. Louis, MO 63130; Telephone: 314-935-3161; Fax: 314-935-4014; lake.s@wustl.edu.

Author contributions statement: C.L.D. and S.P.L. designed the experiments. C.L.D., H.S., J.B., A.J.R., R.M.C., and A.M.C. acquired the data. C.L.D., H.S., and J.B. analyzed the data. C.L.D., J.B., and S.P.L. interpreted the data. C.L.D., J.B., and S.P.L. wrote the manuscript. All authors have read and approved the final submitted manuscript.

Introduction

The elbow is the second most commonly dislocated joint in adults and the most commonly dislocated joint among the pediatric population^{1,2}. Following elbow dislocation, post-traumatic joint contracture (PTJC) is more frequently observed in clinic than joint instability and develops in up to 50% of patients whom experience elbow injury^{1,3}. Range-of-motion less than 100° in flexion-extension has been associated with significant patient-reported functional limitations and patients with post-traumatic elbow contracture often exhibit ~45–65° of motion^{4–8}. Preventing or restoring elbow motion loss can be a difficult, time-consuming and costly challenge because contracture is a multi-tissue pathology and response to treatment is highly variable^{4,9}. Non-surgical (e.g., serial casting, static/dynamic splinting, continuous passive motion) and surgical (e.g., open/arthroscopic soft tissue release) treatment options are used to mitigate motion loss; however, the revision rate for repeat contracture is approximately 20% and elbow range-of-motion rarely returns to pre-injury levels⁷.

Elbow function depends on the integrity of the soft tissues surrounding the joint¹⁰. Clinically, elbow contracture has been attributed to the shortening or fixation of the capsule and ligaments^{9,11}. However, in the clinical setting it is not possible to specifically isolate each of these tissues' mechanical and biological contributions to PTJC. Previously, we developed a rat model of elbow PTJC and showed significant range-of-motion loss in flexion-extension as well as biological changes observed histologically in the anterior capsule (i.e., increased thickness, adhesions, and myofibroblasts) and non-opposing joint surface (i.e., cartilage-capsule interactions indicative of arthrosis) which were consistent with clinical observations^{12–14}. We also showed that muscles/tendons and the anterior capsule contributed approximately 10% and 90% to elbow contracture after 42 days of immobilization, respectively¹⁵. However, after a subsequent period of free mobilization (i.e., unrestricted cage activity), the anterior capsule and ligaments/cartilage were responsible for approximately 26% and 74% of the lost joint motion, respectively¹⁵. While these previous studies identified the tissues which altered joint function, potential changes within these tissues that caused the restricted motion were not examined. The objective of this study was to evaluate the anterior capsule and lateral collateral ligament (LCL) to determine mechanical and biological tissue-specific changes that caused their functional contribution to elbow contracture.

While both the capsule and LCL provide stability to the highly congruent joint surfaces of the elbow, their form and function are different. The capsule is a synovial-lined membrane that encloses the articulating joint surfaces¹¹ and helps resist valgus stress as well as distraction and hyperextension^{6,16}. The LCL extends from the lateral epicondyle of the humerus near the axis of rotation to the crista supinatoris of the ulna¹⁷. The LCL provides varus and rotational stability to the elbow and is primarily loaded during 80–100° of flexion^{17,18}. During elbow dislocation, the capsule and LCL are nearly always injured; our rat model of elbow contracture mimics this damage by surgically inducing an injury to both tissues^{12,13}.

Previous studies in animal models of knee contracture have focused primarily on the capsule, while no previous studies have characterized ligamentous changes due to contracture. In animal models of knee contracture with and without injury followed by immobilization, capsule collagen density was not significantly different in contracted limbs compared to control^{19–21}, but there was a significant decrease in glycosaminoglycan density²¹. Interestingly, in a rabbit model of immobilization-only knee contracture (i.e., no injury), tissue harvested near the joint line of the knee exhibited increased collagen crosslinks in immobilized limbs compared to control²². While insightful, these previous studies in the knee are not generalizable to the elbow because of anatomical and functional differences between these two joints. However, based on this previous work, we hypothesized that a significant increase in tissue volume, as a result of increased extracellular matrix protein deposition, and crosslinking would drive capsule and LCL contribution to elbow contracture in our rat model.

Methods

Animal Model

Male Long-Evans rats (250–350 g, 8–10 weeks old; Charles River Laboratories International) were carefully selected based on anatomical and functional similarities to the human elbow including the presence of a joint capsule, the ability to not only flex-extend but also pronate-supinate, and the ability to use forelimbs in non-weight bearing functions. In this Institutional Animal Care and Use Committee approved study, we used a previously developed injury and immobilization protocol^{12,13}. Briefly, injured animals were anesthetized and unilateral surgery (anterior capsulotomy with LCL transection) was performed followed by immobilization in a flexed position using an external bandage. The control group was neither injured nor immobilized. Elbow periarticular soft tissues (capsule, LCL) were evaluated after 42 days of immobilization (42 IM) to understand changes to these tissues as a result of contracture or after 42 days of immobilization followed by 42 days of free mobilization (42/42 IM-FM) to understand how tissues were altered following joint reloading (Figure 1). The external immobilization bandage was removed for the free mobilization period, and animals were allowed unrestricted cage activity. At each time point, animals were sacrificed via CO₂ inhalation overdose.

LCL Mechanical Testing

After sacrifice at each time point, animals ($n = 8/\text{group}$) were stored immediately in a -20°C freezer. Prior to dissection, animals were thawed for 24 hours and then forelimbs were prepared using methods described previously^{12,13}. Briefly, all skin was removed, the glenohumeral joint was disarticulated, and the paw resected. All surrounding soft tissues (e.g., muscles, tendons, capsule) were removed to isolate the medial and lateral collateral ligaments. The proximal humerus and distal radius/ulna were secured in polycarbonate tubes using hardening putty (Bondo, 3M, Maplewood, MN) as described previously^{12,13}.

A custom mechanical test system was designed and built to evaluate LCL mechanics (Figure 2a). The device used one actuator of a planar biaxial mechanical test system (TestResources, Shakopee, MN) to apply linear displacement and measure force with a single axis load cell

(TestResources). The angle specification platform allowed the joint to be held at a fixed flexion angle during testing. Joints were tested at 90° flexion because a previous study which physiologically loaded human cadaver elbows determined that the LCL was most engaged between 80° to 100° of joint flexion¹⁸. After securing the potted ends of each limb in the custom fixtures of the mechanical test system, the medial collateral ligament was transected so that only the LCL remained intact. A uniaxial ramp-to-failure test was performed at a rate of 0.05 mm/sec, and load was applied perpendicular to the radius/ulna (Figure 2b). Neither preload nor preconditioning was applied to avoid inducing micro-damage to the tissue prior to testing. After testing, the maximum force and stiffness from the ramp-to-failure test were analyzed using a custom written Matlab program (Mathworks, Natick, MA).

LCL Tissue Volume

After sacrifice at each time point, animals ($n = 3/\text{group}$) were stored immediately in a -20°C freezer. Forelimbs were prepared similarly as those for LCL mechanical testing. After the medial and lateral collateral ligaments were isolated, the joints were fixed at 90° flexion with 10% neutral buffered formalin for 72 hours and then stained with 3% phosphomolybdic acid in 70% ethanol for 72 hours to enhance soft tissue contrast. A micro-CT scanner ($\mu\text{CT}40$; ScanCo, Medical, Zurich, CH) was used to scan the forelimbs in 2% agarose inside a 30-mm-diameter tube with the following parameters: $15\ \mu\text{m}^3$ isometric voxel size, 70 kVp x-ray tube potential, 300 ms integration time, and 114 μA x-ray intensity. Dragonfly software (Object Research Systems, Montreal, Quebec) was used to draw regions-of-interest throughout the z-stack of images for each limb to calculate LCL total volume. Due to the complex geometry and the difficulty identifying a consistent landmark to standardize the measurement of the ligament cross-sectional area, the total volume of the LCL was used as a more conservative measurement to normalize the maximum force and stiffness.

Biochemistry

After sacrifice at each time point, capsule ($n = 6/\text{group}$) and LCL ($n = 6/\text{group}$) tissues were immediately isolated, flash frozen in liquid nitrogen, and stored in a -80°C freezer. When ready for analysis, tissues were thawed for five minutes, weighed, and lyophilized for 24 hours. The tissues were then digested in papain solution (1.25 U/mL papain, 0.084 M sodium phosphate, 0.05 M cysteine-HCl, 1% 0.5 M EDTA, 99% H_2O ; pH 6.5) at 65°C for 18 hours. Aliquots of the tissue-papain digest were taken for separate analyses to evaluate collagen and sulfated glycosaminoglycan content via colorimetric assays^{23–25}.

To evaluate collagen content, aliquots of the tissue-papain digest were first diluted with excess papain and hydrolyzed with 4 N NaOH in an autoclave at 122°C and 15 psi for 20 minutes. After the samples returned to room temperature, 4 N HCl was added to neutralize the solution pH. Chloramine-T solution (0.062 M chloramine-T, 20.7% H_2O , 26% isopropanol, 53.3% stock buffer (0.28 M citric acid, 0.85 M sodium acetate, 0.85 M sodium hydroxide, 1.2% acetic acid, 98.8% H_2O)) was added to the samples and incubated at room temperature for 20 minutes. Lastly, Ehrlich's solution (1.17 M Ehrlich's, 70% isopropanol, 30% perchloric acid) was added to the samples and incubated at 65°C for 20 minutes. All samples were evaluated in triplicate on a 96-well plate and read immediately on a spectrophotometer (2300 Multimode Reader, Perkin Elmer, Waltham, MA) at an

absorbance wavelength of 550 nm. Hydroxyproline concentration was calculated based on a linear standard solution of trans-4-hydroxy-L-proline and converted to collagen content by multiplying by 7.46, which reflects the average hydroxyproline composition of collagen in mammalian tissue²⁶.

Aliquots of the tissue-papain digests were plated in triplicate on a 96-well plate and 1,9-dimethylmethylene blue dye (0.029 M sodium formate, 0.050 mM 1,9-dimethylmethylene blue, 0.5% ethanol, 70% H₂O, 29.5% formic acid; pH 3) was added to each sample and read immediately on a spectrophotometer at an absorbance wavelength of 525 nm. The sample sulfated glycosaminoglycan concentration was calculated based on a linear standard solution of chondroitin sulfate.

Collagen Crosslinks

After sacrifice at each time point, capsule ($n = 5/\text{group}$) and LCL ($n = 5/\text{group}$) tissues were immediately isolated, placed into 400 μL phosphate buffered saline, and stored in a -20°C freezer. When samples were ready for analysis, they were first reduced by sodium borohydride (25 mg/mL NaBH₄ in 0.05 M NaH₂PO₄, 0.15 M NaCl; pH 7.4) for one hour on ice followed by 1.5 hours at room temperature to stabilize acid-labile collagen crosslinks. Samples were then hydrolyzed in 6 N HCl at 110°C for 24 hours. The hydrolyzates were precleared by solid phase extraction to remove the bulk of non-crosslinked amino acids (Aspec, Gilson, USA). Dried eluates were re-dissolved in sodium citrate loading buffer (pH 2.2) and analyzed on an amino acid analyzer (Biochrom 30, Biochrom, Great Britain) using a three-buffer gradient system and post column ninhydrin derivatization. The column was eluted at a flow rate of 15 mL/hour at 80°C for (1) five minutes with sodium citrate buffer (pH 4.25), (2) 40 minutes with sodium citrate buffer (pH 5.35), and (3) 20 minutes with sodium citrate/borate buffer (pH 8.6). Retention times of individual crosslinks were established with authentic crosslink compounds. Quantitation was based on ninhydrin generated leucine equivalence factors (DHLNL (dihydroxylysinonorleucine) and HLNL (hydroxylysinonorleucine) = 1.8; HP (hydroxylysyl pyridinoline) and LP (lysyl pyridinoline) = 1.7)²⁷. The number of crosslinks was normalized to the collagen content which was analyzed from an aliquot of hydrolyzed samples to solid phase preclearance.

Statistical Analysis

A two-way ANOVA for time and injury was used to compare all experimental results. When significance was found, post-hoc Bonferroni analyses were used to compare each injured group (42 IM, 42/42 IM-FM) to its respective control (42 FM, 84 FM). Statistical analysis was performed in Prism (GraphPad Prism Software, La Jolla, California) with significance defined as $p < 0.05$.

Results

All animals were included in each analysis (LCL Mechanical Testing: 32/32; LCL Tissue Volume: 12/12; Biochemistry: 24/24; and Collagen Crosslinks: 20/20), no adverse events occurred in any experimental group, and p -values are reported in the plots.

In the three-dimensional tissue volume images, control limb LCLs at 42 and 84 FM exhibited a similar volume and triangular-like geometry (Figure 3a). Injured limb LCLs at 42 IM and 42/42 IM-FM were qualitatively larger structures compared to control. Based on the asymmetric shape of the injured limb LCLs, there appeared to be an irregular deposition of fibrotic tissue or scar with hypertrophy primarily through the midsubstance and around the lateral epicondyle. LCL volume increased significantly with injury; however, only injured limb LCLs at 42/42 IM-FM were significantly increased compared to controls at 84 FM (Figure 3b). Thus, fibrotic scar was not only deposited during immobilization but also throughout the subsequent period of free mobilization.

The LCL maximum force significantly increased with time (Figure 4a). However, the magnitude of change was relatively small and likely caused by overall rat growth due to aging. The rats in this study were classified as young adults (~300 g) and gained weight throughout the study duration as described previously^{12,13,28}. However, this change in rat size was similar for each group and hence there were no significant differences in maximum force between injured or control limb LCLs at either time point (Figure 4a). LCL stiffness only exhibited a significant interaction (Figure 4b). The normalized maximum force significantly decreased with injury, and post-hoc analyses showed that values for injured limb LCLs were significantly decreased at 42 IM and 42/42 IM-FM compared to control (Figure 4c). While normalized stiffness had a significant interaction, it only decreased with injury, and post-hoc analyses exhibited significantly decreased values for injured limb LCLs compared to control at both time points (Figure 4d).

Extracellular matrix protein expression was dependent on the type of tissue, but both exhibited hypertrophy. The total amount of collagen in the capsule significantly increased with injury (Figure 5a); which was consistent with previous joint histology showing increased capsule thickness in injured limbs at 42 IM and 42/42 IM-FM compared to control^{12,13}. However, when collagen content was normalized by wet weight, collagen density in the capsule did not exhibit any significant differences (Figure 5b). Sulfated glycosaminoglycan content and density also did not express any significant changes in the capsule (Figure 5c–d).

LCL collagen content increased significantly with injury, with significantly increased values for injured limbs compared to control at both time points (Figure 6a). Similar to the capsule, collagen density in the LCL also did not exhibit any significant differences (Figure 6b). While the interaction was significant, both sulfated glycosaminoglycan content and density significantly increased in the LCL with time and injury (Figure 6c–d). Sulfated glycosaminoglycan content and density in injured limb LCLs were also significantly increased at 42 IM and 42/42 IM-FM compared to control. The increased collagen and sulfated glycosaminoglycan content in injured limb LCLs compared to control was consistent with the increased LCL tissue volume described earlier (Figure 3b).

The expression of collagen crosslinks was also dependent on the tissue type but exhibited similar trends. Overall, capsule DHLNL and HLNL (immature collagen crosslinks) significantly decreased with time, while HP and LP (mature collagen crosslinks) significantly increased with time (Figure 7a–d). Only DHLNL significantly increased with

injury and exhibited significant increases in injured limb capsules at 42 IM and 42/42 IM-FM compared to control (Figure 7a). Capsule LP significantly decreased with injury but did not exhibit any significant post-hoc comparisons (Figure 7d).

In the LCL, DHLNL and HLNL significantly decreased with time and increased with injury, but only DHLNL expressed a significant interaction (Figure 8a–b). Both immature crosslinks were also significantly increased in injured limb LCLs at 42 IM and 42/42 IM-FM compared to control. While only HP significantly increased with time in the LCL, both HP and LP significantly decreased with injury (Figure 8c–d). Only LP in injured limb LCLs was significantly decreased at both time points compared to control (Figure 8d).

The ratio of immature to mature collagen crosslinks decreased significantly with time in both the capsule and LCL (Figure 9a–b). Only the LCL collagen crosslink ratio significantly increased with injury, but also exhibited a significant interaction, and was significantly increased in injured limbs at 42 IM and 42/42 IM-FM compared to control (Figure 9b).

Discussion

Our previous work showed that the capsule and ligaments/cartilage were the primary periarticular soft tissues that caused the persistent motion loss in our animal model of elbow PTJC¹⁵, so the objective of this study was to evaluate the anterior capsule and LCL to determine tissue-specific mechanical and biological changes that led to their contribution to elbow contracture. Understanding these changes will ultimately help inform the development of tissue targeted treatment strategies. We showed that the increased tissue volume, resulting from increased extracellular matrix protein deposition and collagen crosslinking, likely drives capsule and LCL contribution to elbow contracture in our rat model. While the decreased injured limb LCL mechanics suggest that the deposited proteins were disorganized, additional studies are needed to investigate the impact of tissue organization on elbow contracture.

The total amount of extracellular matrix proteins was altered in both tissues, but the LCL exhibited more significant changes compared to the capsule. The capsule and LCL each exhibited a significant increase in collagen content with injury (Figure 5a, 6a). However, sulfated glycosaminoglycan content was only significantly increased in injured limb LCLs compared to control at both time points (Figure 6c). The increased collagen content in the capsule is supported by previous evidence of capsular thickening observed histologically in the same model of elbow contracture^{12,13}. Significantly increased collagen and sulfated glycosaminoglycan content in injured limb LCLs was also consistent with increased tissue volume (Figure 3). Previous studies in the rabbit knee similarly showed increased ligament cross-sectional area following either immobilization or free mobilization after injury^{29,30}. Overall, increased extracellular matrix proteins were indicative of hypertrophy, likely initiated by a fibrotic wound healing response following injury. Since the articulating surfaces of the elbow are highly congruent, increased tissue volumes in injured limbs likely acted as physical barriers that limited joint motion.

While collagen content increased, there was not a corresponding increase in collagen density for either injured capsules or LCLs compared to control at either time point (Figure 5b, 6b). Animal models of knee contracture showed a similar result^{19–21} and biopsies from patients with pulmonary fibrosis also showed no correlation between collagen density and the degree of fibrosis or tissue stiffness^{31,32}. The capsule also showed no changes in sulfated glycosaminoglycan density, while injured LCLs exhibited a significant but small (~2%) increase at both time points (Figure 5d, 6d). While these results conflict with a rabbit immobilization-only knee contracture model, which reported a decrease in glycosaminoglycan density in immobilized limb capsules compared to control, the tissues in this previous knee model did not experience any injury; thus, protein deposition may differ due to the lack of a wound healing response²¹. The absence of large changes in extracellular matrix protein density in either capsules or LCLs suggests that their contribution to elbow PTJC may be due to the overall increased tissue volume and/or changes to tissue microstructural organization.

Clinically, trauma has been reported to cause abnormal collagen deposition and organization which can impair function and ultimately cause increased adhesions and scar formation³¹. In this study, injured limb LCLs exhibited significantly decreased normalized force and stiffness compared to control at both time points (Figure 4c–d). Thus, the increased LCL tissue volume was weaker compared to control, perhaps because the hypertrophic tissue was disorganized. In animal models of knee contracture, histological evaluation of the capsule from contracted limbs showed that collagen fibers exhibited disordered alignment compared to control^{19,33}. The decreased normalized maximum force and stiffness in injured LCLs could also be partially due to the loading axis evaluated during mechanical testing. The experimental test setup was designed so that the LCL would be primarily loaded along its long axis as it deformed during testing; however, due to the complex geometry and orientation of the LCL, it is possible that the LCL experienced some off-axis loading during the mechanical test. Also, given the large increase in total volume and, hence, the larger joint area covered by the injured LCLs, it is possible that LCL mechanics could decrease in one direction (i.e., on-axis loading), while simultaneously increase or become stiffer in other directions (i.e., off-axis loading) due to the more random deposition of disorganized extracellular matrix proteins.

Crosslinks organize adjacent collagen molecules so collagen fibers can withstand stress³¹. Immature divalent crosslinks, dihydroxylysinonorleucine (DHLNL) and hydroxylysinonorleucine (HLNL), form rapidly as collagen is deposited but decrease as connective tissues mature or age^{32,34}. Mature trivalent crosslinks, hydroxylysyl pyridinoline (HP) and lysyl pyridinoline (LP), are synthesized slowly (~4–6 weeks) and develop over time from immature crosslinks^{32,35,36}. In the current study, the expression of immature and mature collagen crosslinks was similar in both tissues, but the LCL exhibited more significant changes between injured and control. DHLNL was significantly increased in injured limb capsules and LCLs compared to control at both time points, but HLNL was only increased in injured limb LCLs (Figure 7a–b, 8a–b). Increased immature crosslinks in injured limb capsules and LCLs is representative of new collagen synthesis which is consistent with the increased tissue volume and collagen content in both tissues (Figure 3, 5a–b)³⁴. Similarly, in a rabbit model of immobilization-only knee contracture (i.e., no

injury), tissue collected in proximity of the joint line also expressed significantly increased DHLNL and HLNL crosslinks in immobilized limbs compared to control²². In the current study, both mature crosslinks significantly decreased with injury in the LCL, but only LP was decreased in the capsule (Figure 7c–d, 8c–d). The lower expression of HP and LP in injured limb capsules and LCLs indicates that these tissues are less mature compared to control. Thus, the rapid deposition of new collagen following injury causes a build-up of immature LCL tissue, which contributes to the lower normalized maximum force and stiffness exhibited by injured limbs (Figure 4c–d).

The immature to mature collagen crosslink ratio was increased in injured limb LCLs at both time points compared to control, even though the mechanics were decreased (Figure 4c, 9b). Similarly, a study in murine cervical tissue during pregnancy also expressed an increased immature to mature crosslink ratio as well as decreased ultimate stress³⁷. The ratio of immature to mature collagen crosslinks decreased with time in both the capsule and LCL because of significant decreases and increases with time in immature and mature crosslinks, respectively (Figure 9a–b). In animal models of pulmonary fibrosis, DHLNL increased as early as one week after fibrotic insult, while HP increased over 6–10 weeks^{35,38}. Thus, the decreased crosslink ratio after free mobilization potentially relates to the conversion of immature to mature crosslinks, suggesting maturation of the fibrotic scar in the injured limb capsules and LCLs during the period of joint reloading.

Previously, in the same rat model, the capsule and ligaments/cartilage contributed 90% and 10%, respectively, to elbow contracture following immobilization, but after subsequent free mobilization tissue contribution changed to 26% and 74%¹⁵. As discussed above, the LCL often exhibited more significant differences compared to the capsule. Importantly, only after free mobilization was the LCL tissue volume significantly increased and its crosslink ratio indicative of scar maturation (Figure 3b, 9b). However, many other evaluations were significant at both time points. Thus, the results reported herein may partially support the time- and mobilization-dependent tissue contributions; future studies evaluating tissue organization may provide additional understanding.

This study is not without limitations. First, the LCL maximum forces were likely underestimated because the tissue in our test set up was not physiologically loaded and was instead loaded uni-axially with the force applied perpendicular to radius/ulna. However, the LCL mechanical testing set up was optimized to evaluate the LCL at 90° because the LCL was reported to experience the highest loads when oriented between 80–100° flexion during 3D kinematic testing of human cadaver elbows¹⁸. Second, the capsule was not mechanically evaluated because its small size and irregular geometry made it difficult to isolate for tissue-level mechanical testing. Therefore, we previously used the indirect method of sequential dissections to quantify its overall contribution to joint mechanics¹⁵. Third, the biochemical analysis utilized in this study only evaluated bulk collagen changes and did not identify specific types of collagen. Finally, our study did not allow us to determine if these tissue changes were a result of either immobilization or injury. However, we previously showed that an immobilization-only group did not cause persistent elbow contracture and hence was not an appropriate model to evaluate contracture¹³. An injury-only group was not used because (1) after injury, the unstable joint would likely dislocate causing additional

uncontrolled damage and (2) it does not represent how elbow injuries are treated in clinical settings.

Restoring joint motion in post-traumatic elbow contracture is a complex challenge because little is understood about the biological changes in the periarticular soft tissues that drive joint pathology and cause functional deficits. Previous work in our rat model of elbow contracture identified the capsule and LCL as two of the primary tissues contributing to elbow contracture¹⁵. We showed that capsule and LCL contribution to elbow contracture in our rat model resulted from increased tissue volume and immature collagen crosslinks. More significant changes often occurred within the LCL compared to the capsule, identifying the LCL as a potential candidate to target with a tissue specific treatment strategy.

Acknowledgements

Funding was provided by the National Institutes of Health (R03 ARR067504 and R01 AR071444) but did not play a role in the investigation. Aaron M. Chamberlain has received support for work outside of the submitted manuscript from Zimmer-Biomet, DePuy, Arthrex, and Wright Medical. The remaining authors have no conflicts of interest.

References

- [1]. Kuhn MA and Ross G. 2008. Acute elbow dislocations. *Orthopedic Clinics of North America* 39: 155–161.
- [2]. Luukkala T, Temperley D, Basu S, et al. 2018. Analysis of magnetic resonance imaging–confirmed soft tissue injury pattern in simple elbow dislocations. *JSES*.
- [3]. Anakwe RE, Middleton SD, Jenkins PJ, et al. 2011. Patient-Reported Outcomes After Simple Dislocation of the Elbow. *J Bone Joint Surg* 93: 1220–1226. [PubMed: 21776575]
- [4]. Park M, Kim H, and Lee J. 2004. Surgical treatment of post-traumatic stiffness of the elbow. *The Journal of bone and joint surgery British* volume 86: 1158–1162. [PubMed: 15568530]
- [5]. Pederzini LA, Nicoletta F, Tosi M, et al. 2014. Elbow arthroscopy in stiff elbow. *Knee Surg Sports Traumatol Arthrosc* 22: 467–473. [PubMed: 23435987]
- [6]. Bryce CD and Armstrong AD. 2008. Anatomy and biomechanics of the elbow. *Orthopedic Clinics of North America* 39: 141–154.
- [7]. Everding NG, Maschke SD, Hoyer HA, and Evans PJ. 2013. Prevention and treatment of elbow stiffness: a 5-year update. *J Hand Surg Am* 38: 2496–2507. [PubMed: 24210721]
- [8]. Kodde IF, van Rijn J, van den Bekerom MP, and Eygendaal D. 2013. Surgical treatment of post-traumatic elbow stiffness: a systematic review. *JSES* 22: 574–580.
- [9]. Lindenhovius AL and Jupiter JB. 2007. The posttraumatic stiff elbow: a review of the literature. *The Journal of hand surgery* 32: 1605–1623. [PubMed: 18070653]
- [10]. Regan WD, Korinek SL, Morrey BF, and An K-N. 1991. Biomechanical study of ligaments around the elbow joint. *Clin Orthop Relat Res* 170–179.
- [11]. Peacock EE Jr. 1966. Some biochemical and biophysical aspects of joint stiffness: role of collagen synthesis as opposed to altered molecular bonding. *Ann Surg* 164: 1. [PubMed: 5947291]
- [12]. Lake SP, Castile RM, Borinsky S, et al. 2016. Development and use of an animal model to study post-traumatic stiffness and contracture of the elbow. *JOR* 34: 354–364.
- [13]. Dunham CL, Castile RM, Havlioglu N, et al. 2017. Persistent motion loss after free joint mobilization in a rat model of post-traumatic elbow contracture. *JSES* 26: 611–618.
- [14]. Dunham CL, Castile RM, Havlioglu N, et al. 2018. Temporal Patterns of Motion in Flexion-extension and Pronation-supination in a Rat Model of Posttraumatic Elbow Contracture. *Clinical Orthopaedics and Related Research* 476: 1878–1889. [PubMed: 30001292]

- [15]. Dunham CL, Castile RM, Chamberlain AM, and Lake SP. 2019. The Role of Periarticular Soft Tissues in Persistent Motion Loss in a Rat Model of Posttraumatic Elbow Contracture. *JBJS*101: e17.
- [16]. Safran MR and Baillargeon D. 2005. Soft-tissue stabilizers of the elbow. *JSES* 14: S179–S185.
- [17]. King GJ, Morrey BF, and An K-N. 1993. Stabilizers of the elbow. *JSES*2: 165–174.
- [18]. Olsen BS, Michael T, Søjbjerg JO, et al. 1996. Lateral collateral ligament of the elbow joint: anatomy and kinematics. *JSES*5: 103–112.
- [19]. Steplewski A, Fertala J, Beredjikian PK, et al. 2016. Auxiliary proteins that facilitate formation of collagen-rich deposits in the posterior knee capsule in a rabbit-based joint contracture model. *JOR*34: 489–501.
- [20]. Ando A, Suda H, Hagiwara Y, et al. 2012. Remobilization does not restore immobilization-induced adhesion of capsule and restricted joint motion in rat knee joints. *The Tohoku journal of experimental medicine*227: 13–22. [PubMed: 22510696]
- [21]. Akeson WH, Amiel D, and Woo SL. 1980. Immobility effects on synovial joints. The pathomechanics of joint contracture. *Biorheology*17: 95–110. [PubMed: 7407354]
- [22]. Akeson W, Amiel D, Mechanic G, et al. 1977. Collagen cross-linking alterations in joint contractures: changes in the reducible cross-links in periarticular connective tissue collagen after nine weeks of immobilization. *Connect Tissue Res*5: 15–19. [PubMed: 141358]
- [23]. Cissell DD, Link JM, Hu JC, and Athanasiou KA. 2017. A modified hydroxyproline assay based on hydrochloric acid in Ehrlich's solution accurately measures tissue collagen content. *Tissue Engineering Part C: Methods*23: 243–250. [PubMed: 28406755]
- [24]. Reddy GK and Enwemeka CS. 1996. A simplified method for the analysis of hydroxyproline in biological tissues. *Clinical biochemistry* 29: 225–229. [PubMed: 8740508]
- [25]. Farndale RW, Sayers CA, and Barrett AJ. 1982. A direct spectrophotometric microassay for sulfated glycosaminoglycans in cartilage cultures. *Connect Tissue Res*9: 247–248. [PubMed: 6215207]
- [26]. Neuman RE and Logan MA. 1950. The determination of collagen and elastin in tissues. *Journal of Biological Chemistry* 186: 549–556.
- [27]. Avery NC, Sims TJ, and Bailey AJ. 2009. In: editors. *Extracellular Matrix Protocols*. Springer; p 103–121.
- [28]. Sengupta P. 2013. The laboratory rat: relating its age with human's. *Int J Prev Med*4: 624. [PubMed: 23930179]
- [29]. Bray R, Shrive N, Frank C, and Chimich D. 1992. The early effects of joint immobilization on medial collateral ligament healing in an ACL-deficient knee: a gross anatomic and biomechanical investigation in the adult rabbit model. *JOR*10: 157–166.
- [30]. Loitz-Ramage BJ, Frank CB, and Shrive NG. 1997. Injury size affects long term strength of the rabbit medial collateral ligament. *Clinical Orthopaedics and Related Research*@337: 272–280.
- [31]. Nimni ME. 1983. Collagen: structure, function, and metabolism in normal and fibrotic tissues. *Semin Arthritis Rheum*13: 1–86. [PubMed: 6138859]
- [32]. Jones MG, Andriotis OG, Roberts JJ, et al. 2018. Nanoscale dysregulation of collagen structure-function disrupts mechano-homeostasis and mediates pulmonary fibrosis. *eLife*7: e36354. [PubMed: 29966587]
- [33]. Trudel G, Laneuville O, Coletta E, et al. 2014. Quantitative and temporal differential recovery of articular and muscular limitations of knee joint contractures; results in a rat model. *Journal of Applied Physiology*117: 730–737. [PubMed: 25123199]
- [34]. Eyre DR, Paz MA, and Gallop PM. 1984. Cross-linking in collagen and elastin. *Annu Rev Biochem*53: 717–748. [PubMed: 6148038]
- [35]. Last JA, King T, Nerlich A, and Reiser KM. 1990. Collagen cross-linking in adult patients with acute and chronic fibrotic lung disease. *Am Rev Respir Dis*141: 307–13. [PubMed: 2301849]
- [36]. Eekhoff JD, Fang F, and Lake SP. 2018. Multiscale mechanical effects of native collagen cross-linking in tendon. *Connect Tissue Res*59: 410–422. [PubMed: 29873266]

- [37]. Yoshida K, Jiang H, Kim M, et al.2014. Quantitative evaluation of collagen crosslinks and corresponding tensile mechanical properties in mouse cervical tissue during normal pregnancy. PLoS One9.
- [38]. Reiser KM, Tryka AF, Lindenschmidt RC, et al.1986. Changes in collagen cross-linking in bleomycin-induced pulmonary fibrosis. J Biochem Toxicol1: 83–91.

Author Manuscript

Author Manuscript

Author Manuscript

Author Manuscript

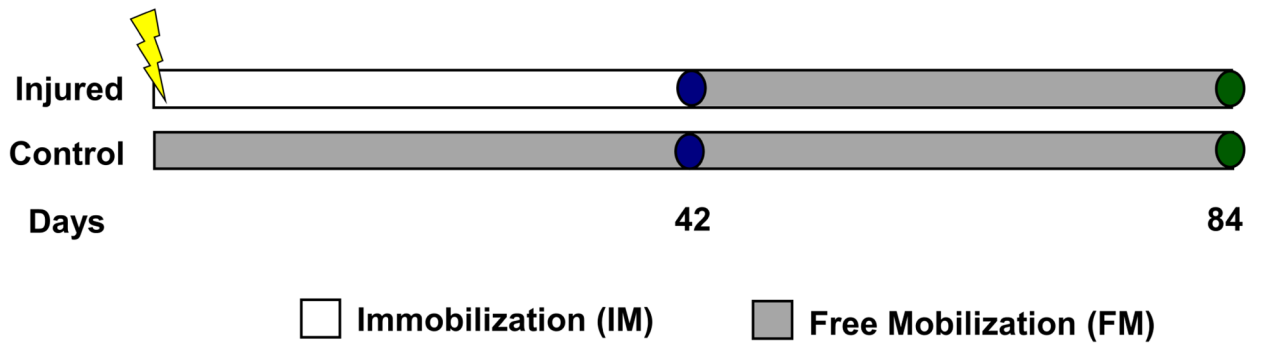


Figure 1.
The timeline describes the experimental evaluation for injured and control animals (lightning bolt = surgery, oval = time point).

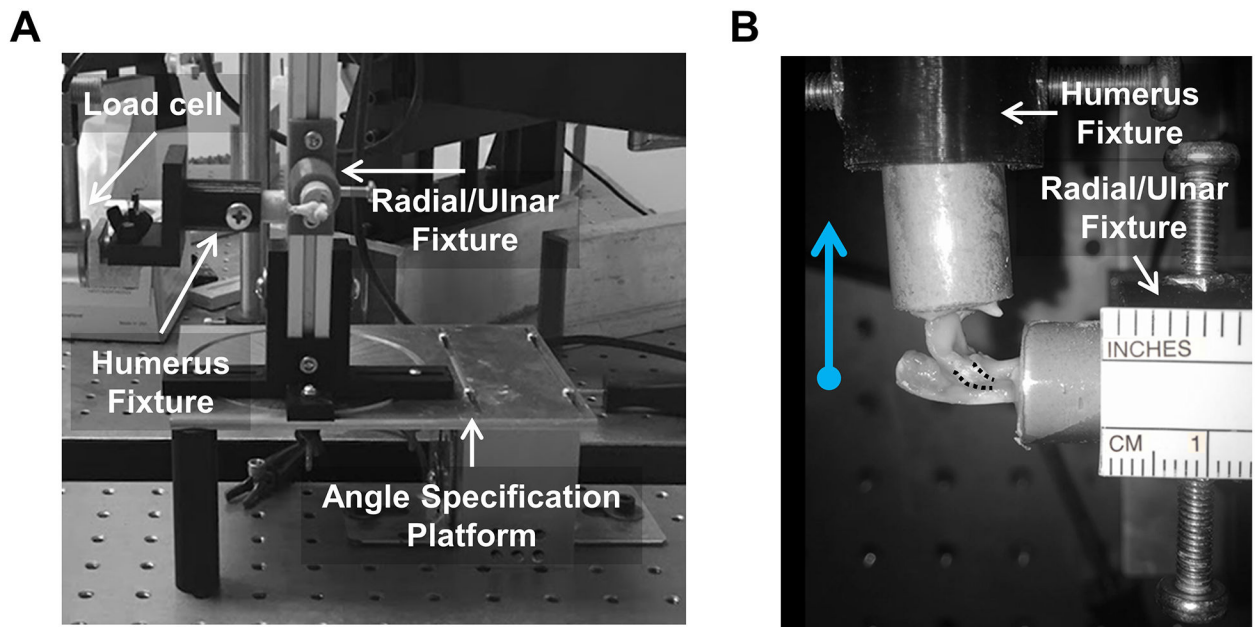


Figure 2. (A) The biomechanical test system to evaluate the lateral collateral ligament (LCL) with the joint held fixed at 90° flexion. (B) The load from the linear actuator was applied perpendicular to the radius/ulna (LCL outlined with the dotted lines).

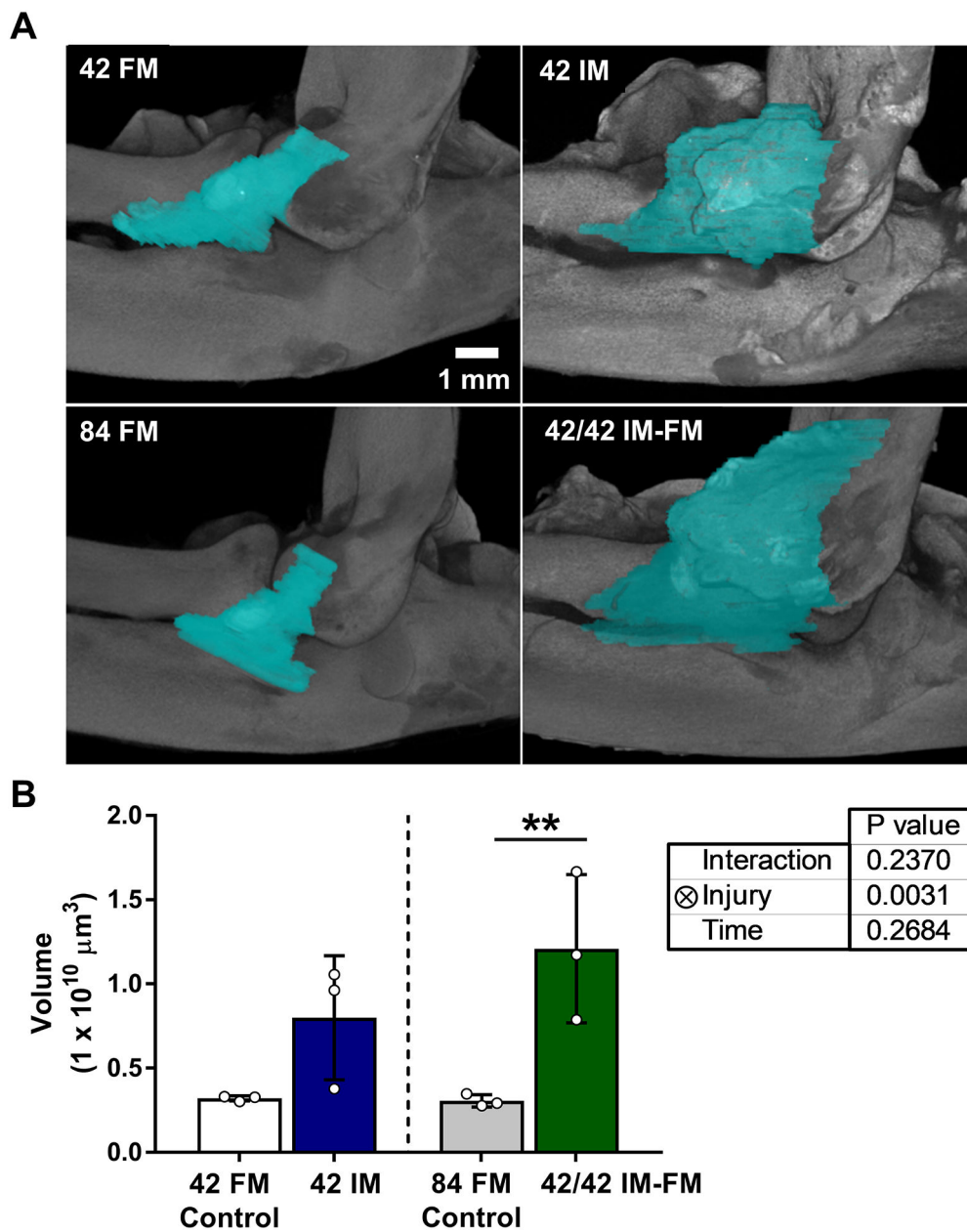


Figure 3.
 (A) Contrast enhanced micro-computed tomography three-dimensional images representative of injured and control limbs at each time point with the lateral collateral ligament (LCL) pseudo-colored aqua (scale bar = 1 mm). (B) LCL tissue volume increased with injury (average \pm standard deviation; $**p < 0.01$).

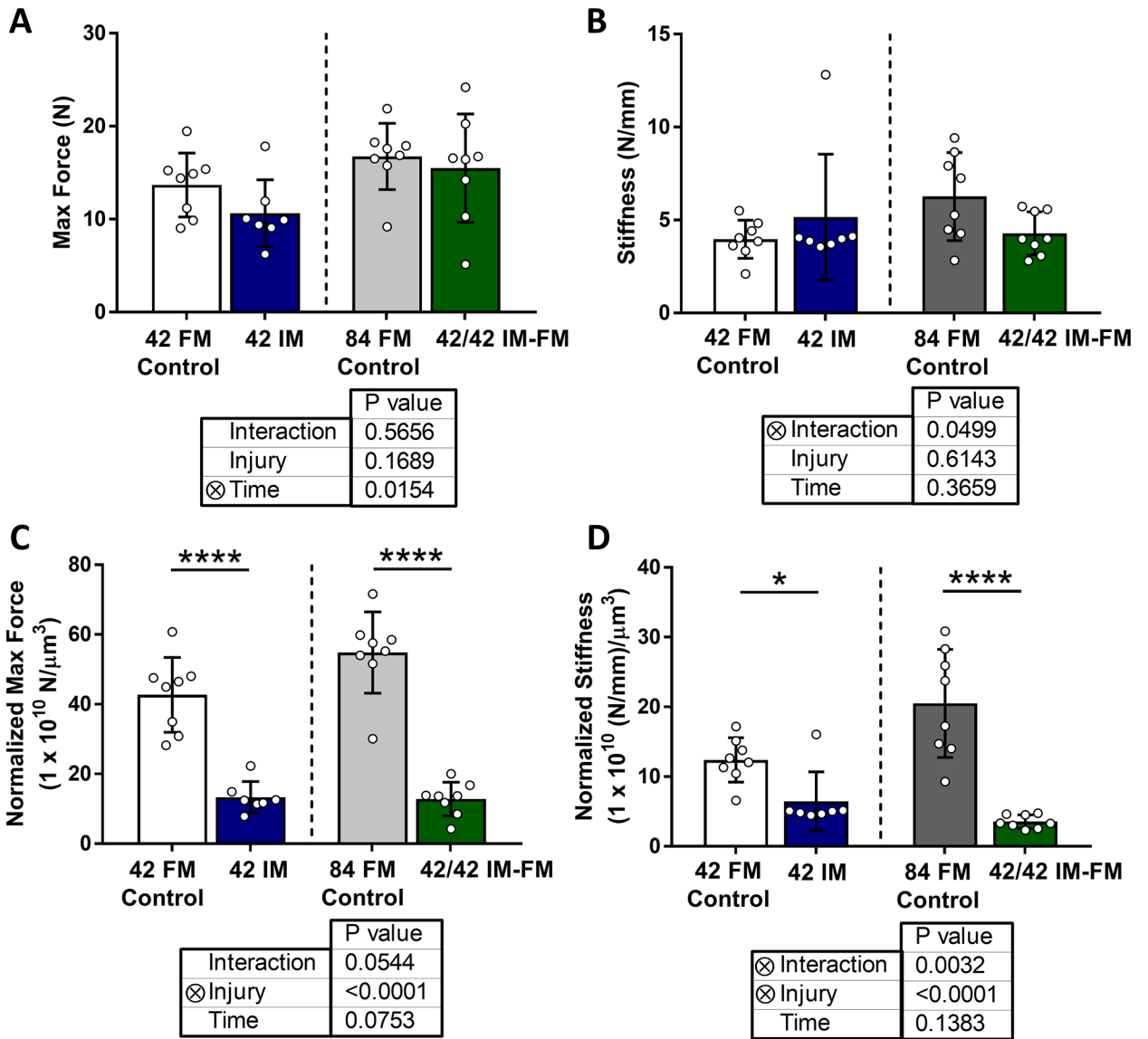


Figure 4. Lateral collateral ligament (A) maximum force increased with time, (B) stiffness exhibited significant interaction between factors, (C) normalized maximum force (maximum force/tissue volume) decreased with injury, and (D) normalized stiffness (stiffness/tissue volume) decreased with injury and had significant interaction between factors (average \pm standard deviation; * $p < 0.05$, **** $p < 0.0001$).

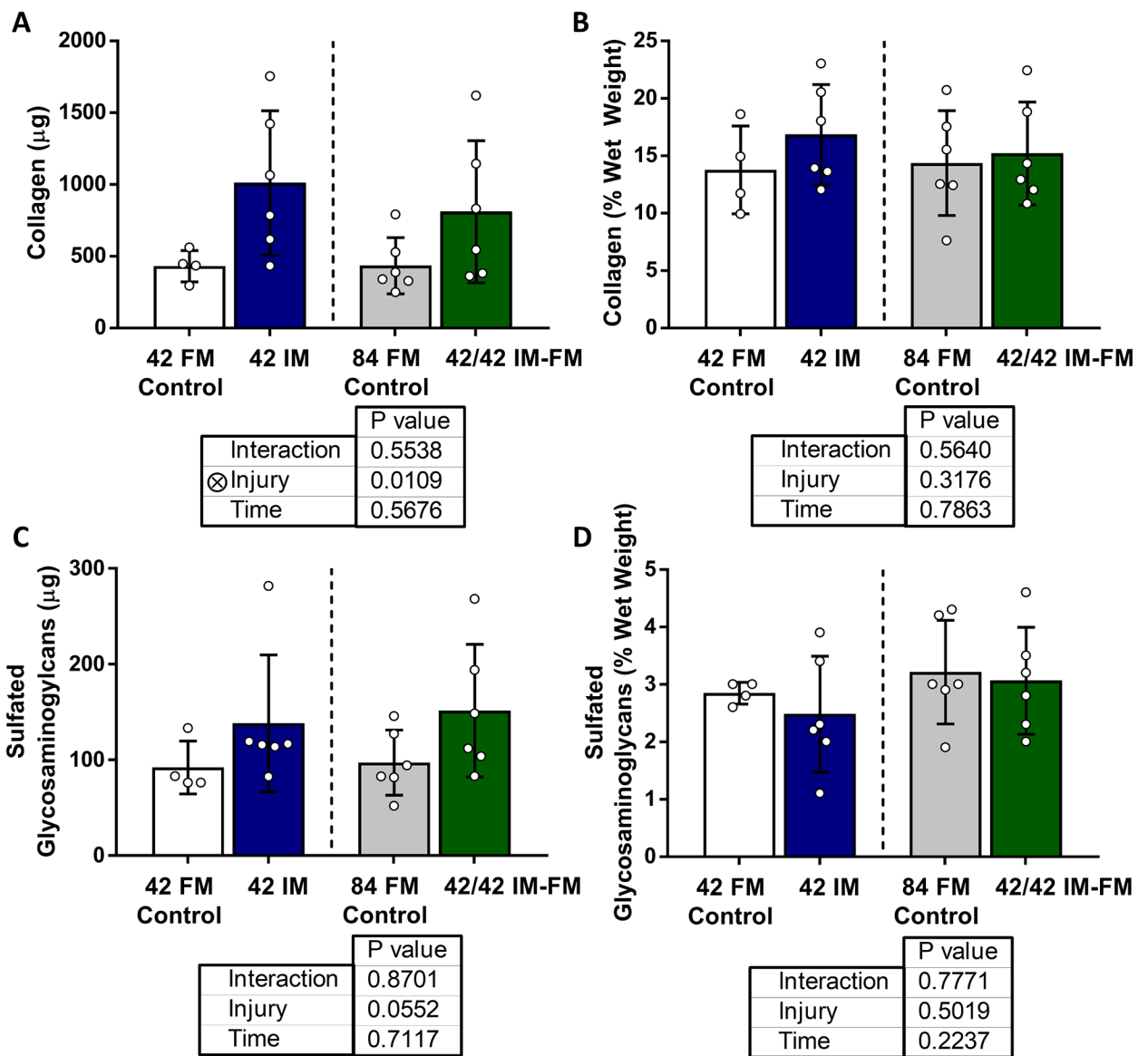


Figure 5. Capsule: (A) Collagen content increased with injury, however, (B) collagen density (collagen content/tissue wet weight), (C) sulfated glycosaminoglycan content, and (D) sulfated glycosaminoglycan density (sulfated glycosaminoglycan content/tissue wet weight) did not exhibit significant differences (average \pm standard deviation).

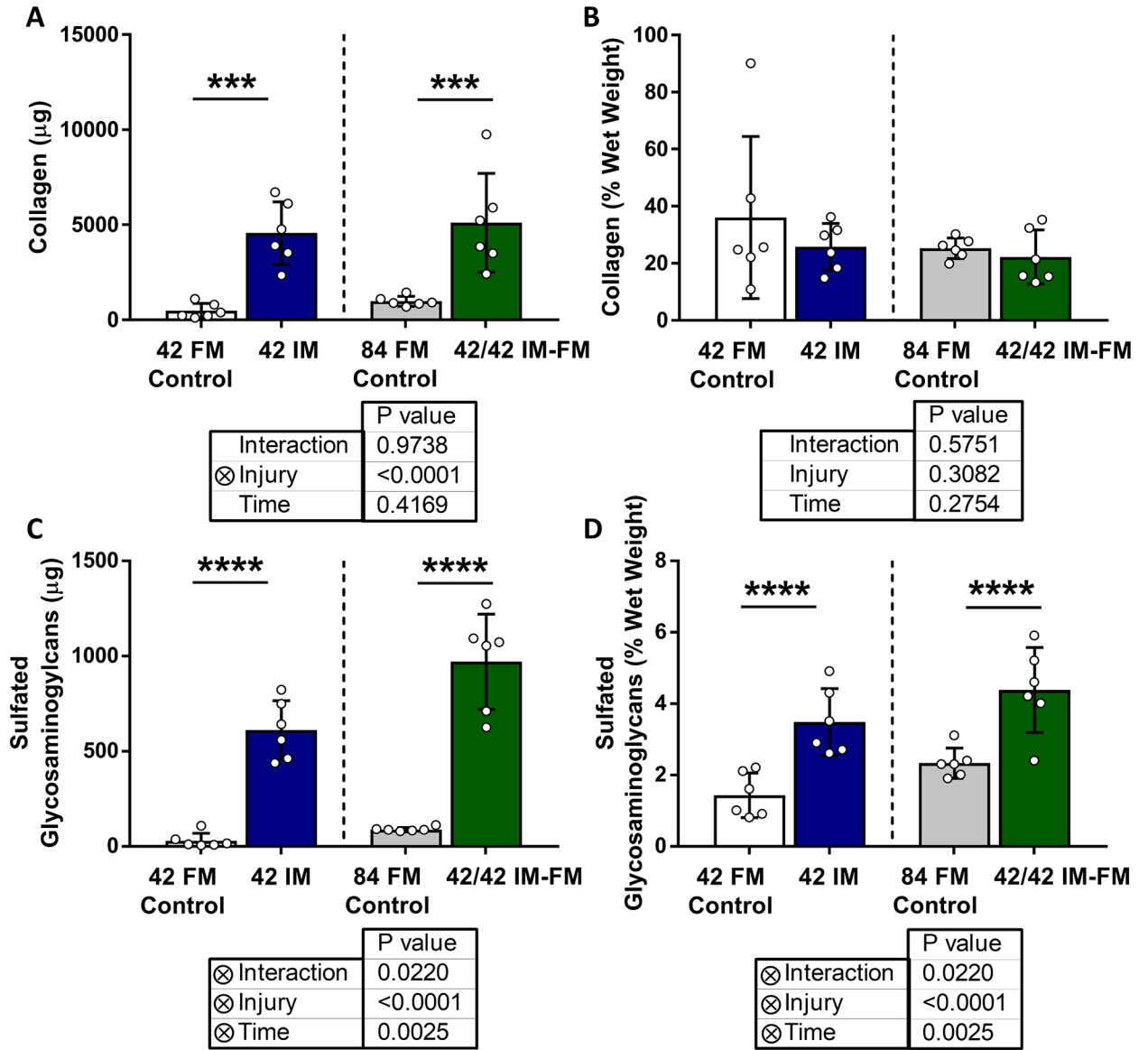


Figure 6. Lateral collateral ligament: (A) Collagen content increased with injury, but (B) collagen density (collagen content/tissue wet weight) did not exhibit any significant differences. (C) Sulfated glycosaminoglycan content and (D) density (sulfated glycosaminoglycan content/tissue wet weight) increased with injury and time, but also had a significant interaction between these two factors (average \pm standard deviation; *** $p < 0.001$, **** $p < 0.0001$).

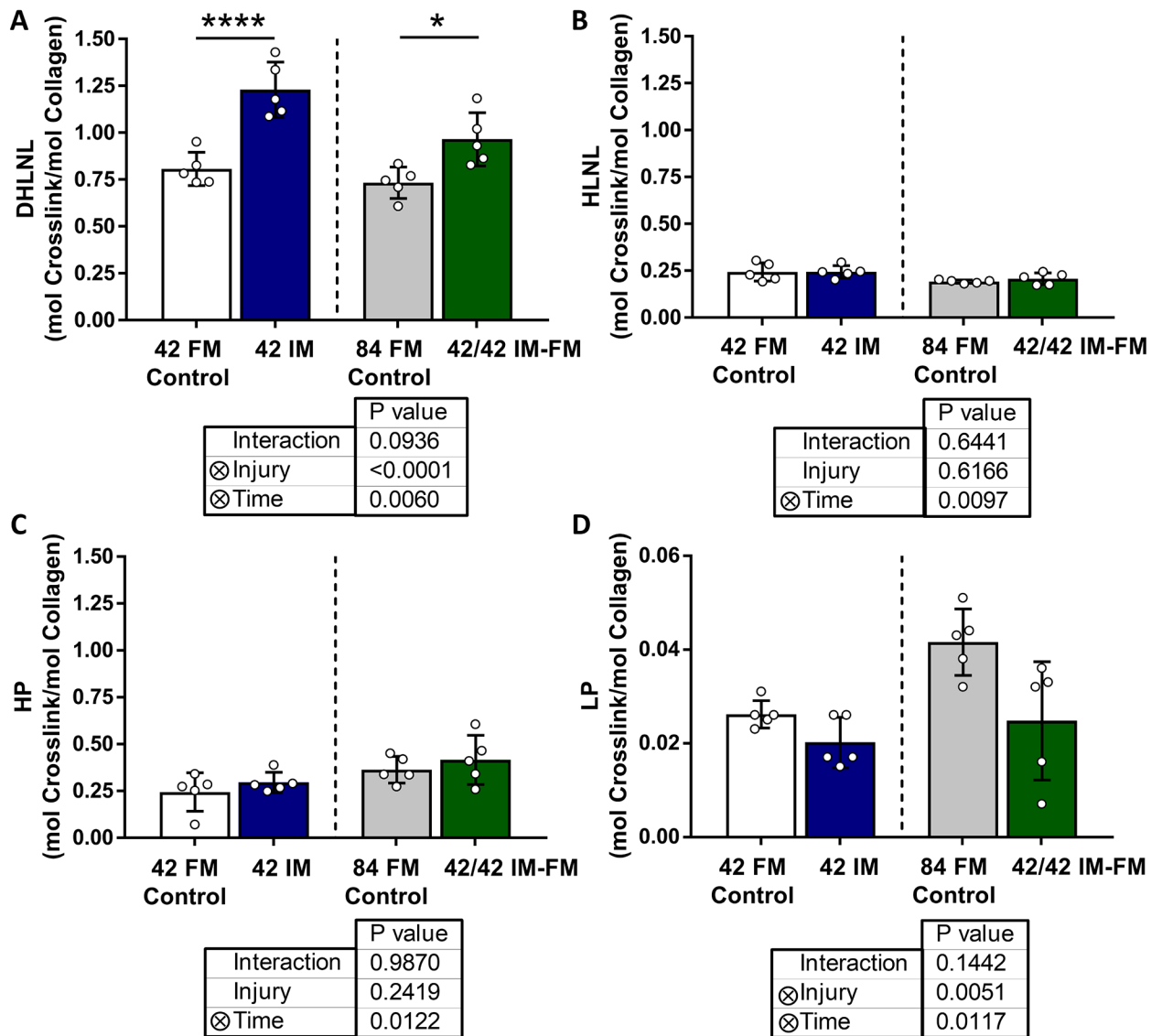


Figure 7. Capsule: Immature collagen crosslinks, (A) DHLNL and (B) HLNL, decreased with time and only DHLNL increased with injury. Mature collagen crosslinks, (C) HP and (D) LP, increased with time and only LP decreased with injury (average ± standard deviation; * $p < 0.05$, **** $p < 0.0001$).

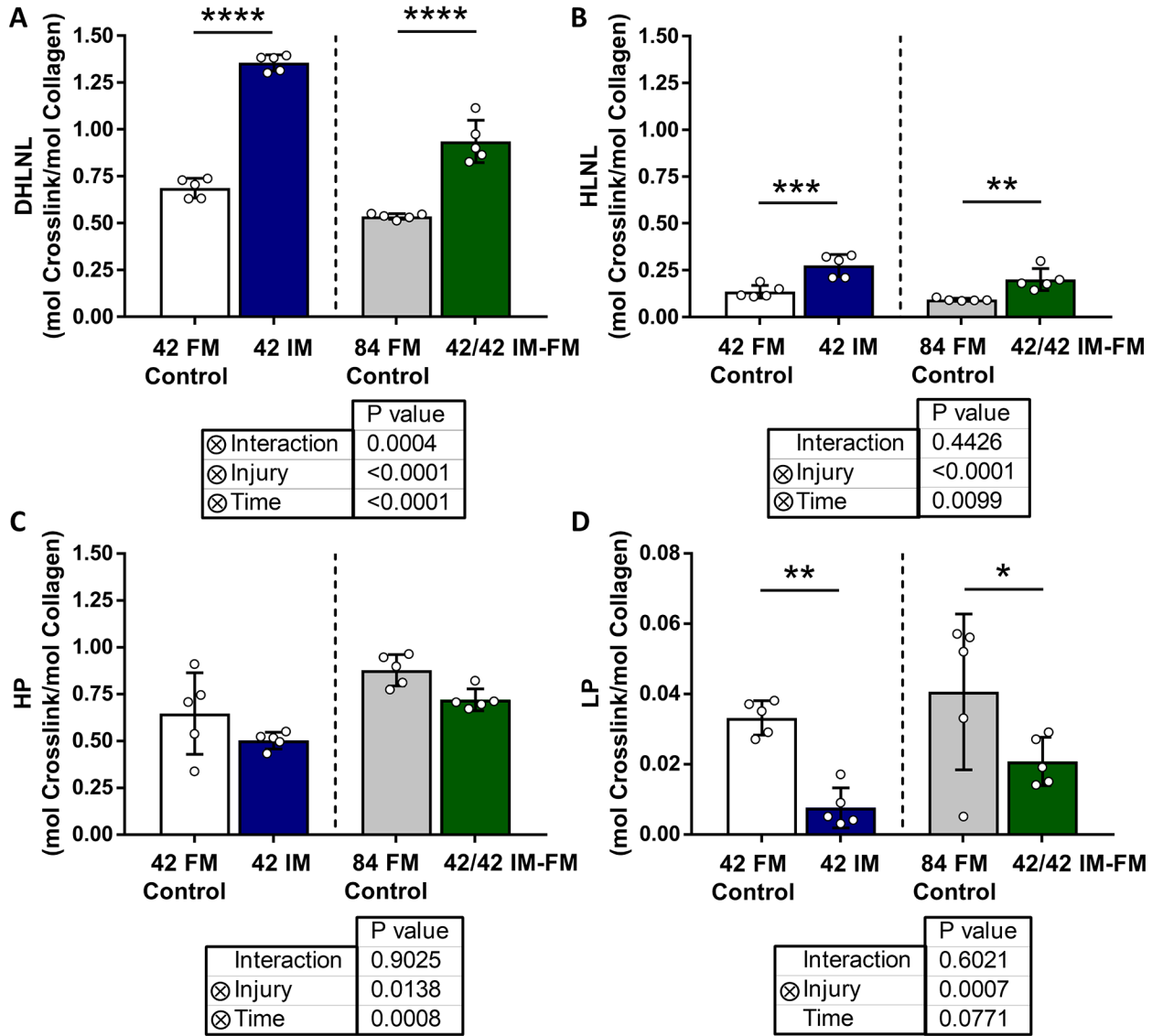


Figure 8. Lateral collateral ligament: Immature collagen crosslinks, (A) DHLNL and (B) HLNL, decreased with time and increased with injury. Only DHLNL exhibited a significant interaction between these two factors. Mature collagen crosslinks, (C) HP and (D) LP, decreased with injury and only HP increased with time (average \pm standard deviation; * $p < 0.05$, ** $p < 0.01$, *** $p < 0.001$, **** $p < 0.0001$).

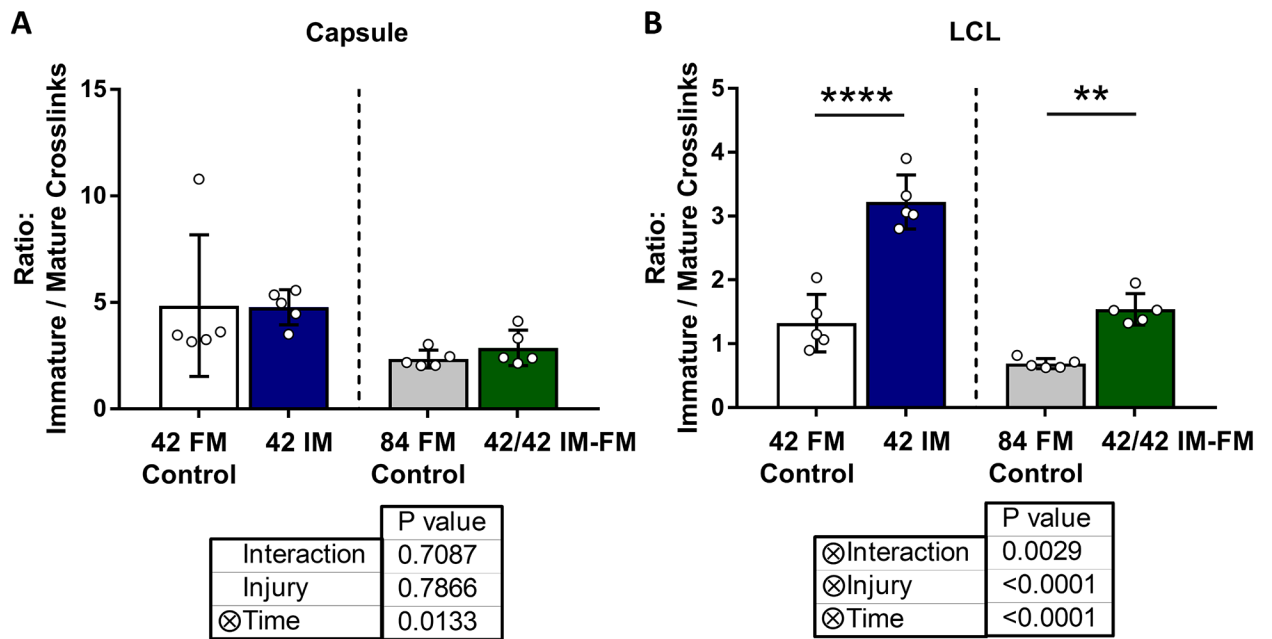


Figure 9. Immature to mature collagen crosslink ratio ((DHLNL+HLNL)/(HP+LP)) decreased with time in the (A) capsule and (B) lateral collateral ligament (LCL). Only the LCL increased with injury and had a significant interaction between the two factors, injury and time (average \pm standard deviation; ** $p < 0.01$, **** $p < 0.0001$).